Size dependence of refractive index of Si nanoclusters embedded in SiO_2

J. A. Moreno, B. Garrido,[a] P. Pellegrino,[b] C. Garcia, J. Arbiol, and J. R. Morante
Department d'Electrònica, Universitat de Barcelona, Martí Franquès, 1, 08028 Barcelona, Spain

P. Marie, F. Gourbilleau, and R. Rizk
Structure des Interfaces et Fonctionnalité des Couches Minces (SIFCOM) Unite Mixte de Recherche (UMR) Centre National de la Recherche Scientifique (CNRS) 6176, Ecole Nationale Supèrieure d'Ingènieurs de Caen (ENSICAEN), 6 Boulevard Maréchal-Juin, F-14050 Caen Cedex, France

(Received 11 January 2005; accepted 5 May 2005; published online 8 July 2005)

The complex refractive index of SiO_2 layers containing Si nanoclusters (Si-nc) has been measured by spectroscopic ellipsometry in the range from 1.5 to 5.0 eV. It has been correlated with the amount of Si excess accurately measured by x-ray photoelectron spectroscopy and the nanocluster size determined by energy-filtered transmission electron microscopy. The Si-nc embedded in SiO_2 have been produced by a fourfold Si^+ ion implantation, providing uniform Si excess aimed at a reliable ellipsometric modeling. The complex refractive index of the Si-nc phase has been calculated by the application of the Bruggeman effective-medium approximation to the composite media. The characteristic resonances of the refractive index and extinction coefficient of bulk Si vanish out in Si-nc. In agreement with theoretical simulations, a significant reduction of the refractive index of Si-nc is observed, in comparison with bulk and amorphous silicon. The knowledge of the optical properties of these composite layers is crucial for the realization of Si-based waveguides and light-emitting devices. © *2005 American Institute of Physics*. [DOI: 10.1063/1.1943512]

I. INTRODUCTION

Composite materials containing silicon nanocrystals or nanoclusters (Si-nc) in a silicon oxide matrix are attractive for several reasons. They present tunable photo- and electroluminescence in the visible region and recently, relatively efficient light-emitting devices (LEDs) have been demonstrated.[1] The recent observation of optical gain in these materials provides a breakthrough, as they can be used to ensure optical amplification in an integrated waveguide.[2,3] Combined with electronic injection in the LEDs, this result suggests to pursue a silicon injection laser. Moreover, an efficient energy transfer between Si-nc to Er^{3+} ions in silica-based materials has also been demonstrated, so that small-size, highly performing, and low cost waveguide amplifiers can be devised working in the 1.54-μm window of the optical fibers.[4,5]

The knowledge of the relationship between the structural properties and the complex refractive index of the composite is crucial for the design of optically active layers in optoelectronic and photonic applications. For example, the accurate control of refractive index contrast between the active material containing Si-nc and the cladding layers is a fundamental requirement for best energy confinement of the guided modes. Moreover, it has been theoretically demonstrated, and to some extent by experiments, that the static refractive index of Si-nc is quite different to that of bulk crystalline Si and strongly depends on the average size of the nanostructures.[6,7] With the objective of providing useful data of the interplay between structural and optical properties, this work aims at the determination and modeling of the complex refractive index—between 1.5 and 5 eV—of silicon oxides containing Si-nc of different sizes. A few works exist in literature dealing with the refractive index of composite layers with Si-nc, obtained by cosputtering[8,9] or laser pyrolisis.[10] However, these studies refer to less compact layers than the ones we used, so their modeling is complicated by the presence of a third phase, voids. Furthermore, we provide accurate results regarding the correlation of the optical modeling with the size of the nanostructures, as determined by energy-filtered transmission electron microscopy (EFTEM). The Si-nc has been obtained by Si ion implantation in SiO_2 and the thermal processing conditions have been optimized to obtain Si-nc with average sizes between 3 and 5 nm, which is the best range to have efficient luminescent emission in the visible, as well reported in literature.[11,12]

II. EXPERIMENTS

Silicon oxides (2 μm thick) thermally grown on Si were used as substrates. A fourfold Si ion implantation was performed to obtain a flat profile of Si excess. This constant profile aims at a straightforward modeling of the spectroscopic ellipsometry experiments. Calculations with the SRIM2000 simulator were carried out in order to obtain the implanted Si profile versus depth. Three samples (labeled hereafter as A, B, and C) were fabricated with nominal excess of 5%, 10%, and 15%, respectively. The Si-nc phase was precipitated after annealing the samples at 1100 °C up to 4 h in N_2 atmosphere. We have previously shown in similar samples that this long annealing makes basically the whole Si excess to precipitate and form silicon nanocrystals of about 3–5 nm of average diameter, with stable and well-passivated interface with the matrix.[11,12]

[a]Electronic mail: blas@el.ub.es
[b]Electronic mail: paolo@el.ub.es

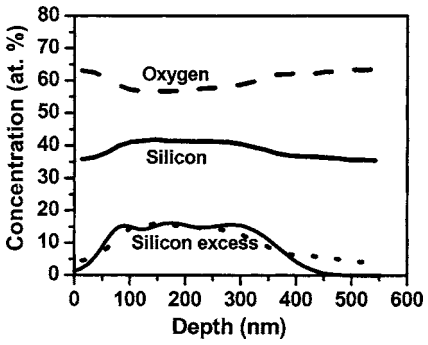

FIG. 1. Concentration profiles for sample C. Simulated profile of Si excess (full line) is also included (in arbitrary units) for comparison.

Silicon excess was accurately measured by x-ray photoelectron spectroscopy (XPS) experiments. The composition profiles were determined by sputtering the samples with an argon gun while carrying out the XPS measurements. Figure 1 shows the typical concentration profiles obtained for sample C and the simulated Si excess profile after correcting the SRIM values for the increased Si content and the introduction of additional matter (swelling). The experimental Si excess profile (dotted line) qualitatively matches the simulated one (full line). The stoichiometric ratio $x=[O]/[Si]$ is defined in correspondence to the formula SiO_x and the actual silicon excess as $[Si]_{excess}=y=(1-0.5[O])$, i.e., $y=(1-x/2)/(1+x)$ (to avoid confusion upon the definition of Si excess); both of them were easily calculated from XPS measurements. The experimentally estimated values of x, y for samples A, B, and C are summarized in Table I.

III. RESULTS

The EFTEM observations aimed to image the layer with Si-nc and monitor the Si-nc size distribution. They were performed by means of a field emission of 200-kV Jeol 2010F equipped with a Gatan image filter (GIF 2000) which adds electron-energy-loss spectroscopy (EELS) and filtering imaging capabilities. We energetically filtered the EELS spectra by using the GIF, around the Si plasmon (placed at 17 eV), which is sufficiently separated from the SiO_2 plasmon (at about 26 eV).

The Si-nc average size does not show a depth dependence, while the thickness of the Si-nc rich oxide layer does not vary with the implanted dose, in accordance with the simulation of a flat profile aimed by the multi-implantation scheme. Thus, from the images we determined that the in-depth structure consists of a superficial, 50-nm-thick, SiO_2 layer depleted of Si-nc, and a buried, Si-nc rich, region with a thickness of about 275 nm. Moreover, a systematic increase of the mean size of the Si-nc with increasing Si excess was observed. Average diameters from 3.6 to 4.6 nm were obtained for a Si excess varying from 7% to 13% (see Table I), values which are significantly higher than others reported from conventional or high-resolution electron microscopy for similar Si excess.[1,10,12] We attribute this difference to the fact that EFTEM allows to image both crystalline and amorphous phases. By assuming an almost complete phase separation between excess Si and SiO_2 (corroborated by Raman and infrared measurements, not shown)[13] and by combining the values of Si excess and particle size, we obtain an estimated density of about 4×10^{18} Si-nc/cm^3, which surprisingly we found independent of the Si excess value.

TABLE I. Compositional data and mean diameter (with standard deviation) of samples with different Si excess concentrations.

Sample lable	Measured Si excess y (at. %)	[O]/[Si] ratio x	Mean diameter (nm)
A	7	1.63	3.6±0.4
B	9.5	1.50	4.1±0.5
C	13	1.38	4.6±0.6

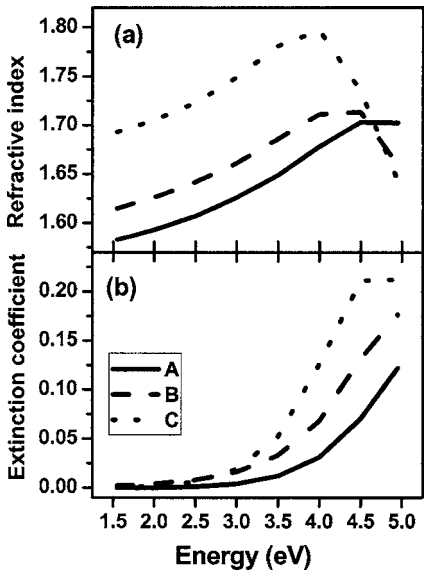

FIG. 2. Refractive index (a) and extinction coefficient (b) of composite samples A, B, and C measured by spectroscopic ellipsometry.

The complex refractive index of the composite layers was measured by spectroscopic ellipsometry, taking into account the multilayer sequence indicated above for modeling the data. The refractive index (real part) and extinction coefficient (imaginary part) are shown in Fig. 2 for samples A, B, and C. In the low-energy (1.5–1.9 eV) side of the measured spectrum, where the absorption is negligible, we have found a parabolic dependence of the refractive index with Si excess, and this result is displayed in Fig. 3 for an energy of 1.96 eV ($\lambda=632$ nm). Such dependence allows to interpolate composition values for a target refractive index and has been independently corroborated by *m*-lines measurements at the same wavelength on planar waveguides fabricated from the same material.[13] These values for the refractive index are about 7% higher than those obtained by Charvet *et al.* for similar Si excess in layers grown by sputtering.[9] The higher compactness of the samples studied here can account for such a variation. Amans *et al.* obtain similar values to ours for their pyrolized samples, once they have corrected for more than 50% of porosity.[10]

The complex refractive index of the Si-nc can be extracted from the experimental results shown in Fig. 2. For this purpose, we have used the modeling involved in the

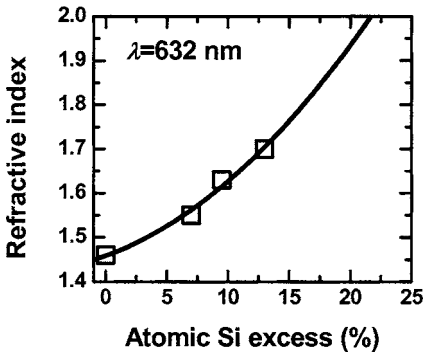

FIG. 3. Refractive index of samples A, B, and C measured by ellipsometry at 632 nm. The data fit very well to a quadratic function for moderate Si excess content (dotted curve).

Bruggeman effective-medium approximation (EMA).[14,15] The composite material is modeled as having two phases with volume fractions f and $1-f$, respectively. In the case of our samples they have been determined from the concentration of nanocrystals indicated in Table I and the material densities of Si and SiO_2. If we call ε_{nc}, ε_{compo}, and ε_{oxide} to the dielectric functions of the Si-nc, the composite, and the oxide, respectively, the only unknown variable in the following equation is the dielectric function of the Si-nc:

$$f\frac{\varepsilon_{nc}-\varepsilon_{compo}}{\varepsilon_{nc}+2\varepsilon_{compo}}+(1-f)\frac{\varepsilon_{oxide}-\varepsilon_{compo}}{\varepsilon_{oxide}+2\varepsilon_{compo}}=0. \quad (1)$$

From the complex dielectric function of the Si-nc we have calculated their refractive index and extinction coefficient, which are shown in Fig. 4 for samples A, B, and C. For the sake of comparison, in the same figure we have also plotted the refractive index and extinction coefficients of crystalline bulk Si and amorphous Si and those of the Si-nc obtained by laser pyrolisis by Amans *et al.*[10] The refractive index of bulk

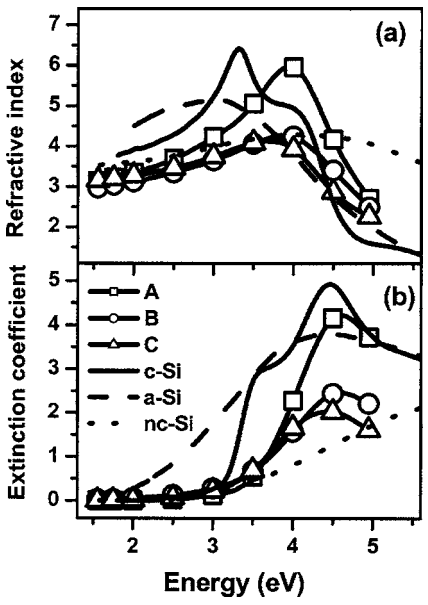

FIG. 4. Refractive index (a) and extinction coefficient (b) of Si nanocrystals calculated from Bruggeman effective-medium approximation. Those corresponding to crystalline Si, amorphous Si, and Si nanocrystals obtained by laser pyrolisis (from literature) are also included for comparison.

Si clearly shows the E_0', E_1, and E_2 transitions at 3.3, 3.5, and 4.3 eV, respectively, which are related to the maxima of the joint density of states for the valence and conduction bands.[16] On the contrary the refractive index of Si-nc increases steadily with energy, and is featureless in the region around the E_0' and E_1 transitions before reaching a maximum at approximately 4.0 eV, near the E_2 transition in bulk Si. The refractive index is lower for Si-nc in the whole studied energy range, as already observed in previous experimental studies of sputtered[8,9] and laser-pyrolized[10] samples, and this fact is in agreement with the theoretical studies of Lannoo *et al.*[7] for the static dielectric constant of Si-nc in comparison with bulk Si. The extinction coefficient of Si-nc is lower than that of crystalline and amorphous Si and also increases with energy and peaks at 4.5 eV, close to the E_2 resonance.

Amorphous silicon (a-Si) only exhibits one broad resonance covering the region of E_0', E_1, and E_2 transitions, as can be seen in Fig. 4. Similarly, Si-nc show a unique resonance with energy, but shifted to high energy and centered at 4.5 eV, near the E_2 resonance of bulk Si. The amount of this "blueshift" correlates with the size of the Si-nc and can be considered as a direct consequence of quantum confinement effects. The fact that the refractive index of Si-nc is smooth and featureless like that of amorphous silicon can be a consequence of the very wide size distribution (dispersion $2\sigma = 1.2$ nm) and the random orientation of the clusters.

The values obtained for the refractive index and extinction coefficient of the Si-nc phase for the two samples with large Si-nc—samples B (4.1 nm) and C (4.6 nm)—are similar to each other and also quite similar to the results reported in literature for samples with similar Si-nc average size,[9,10] so this is a strong indication of consistency. Regarding sample A, the one with the smaller Si-nc (3.6 nm), the refractive index and extinction coefficient are similar to those of samples B and C at low energies (visible range). Nevertheless, on the high-energy side, above 3.0 eV, sample A presents a more pronounced peak at 4.0 eV, being quantitatively closer to bulk Si. This is surprising as one would expect that for large Si-nc the refractive index would be closer to that of bulk Si.

A possible explanation for this discrepancy must take into account the modeling, the composition, and the structure. First of all, the Bruggeman model for mixing is more precise if both phases have a similar volume fraction, which is the case for samples B and C. Furthermore, one should take into account that the compositional transition between the nanocrystal and the matrix is not abrupt. The transition region has been shown as a thin shell of suboxides, which will depend very much on processing conditions.[17] However, the explanation for the pronounced difference seems to come from the amorphous or crystalline nature of the Si-nc. From high-resolution TEM we have determined that all three samples have a population of crystalline precipitates with a mean size of about 2.6 nm (±1.1). The EFTEM cannot distinguish between amorphous or crystalline precipitates, so we conclude that a significant part of the large Si-nc have an amorphous character or, more probably, an amorphous outer shell. Thus, those results strongly suggest that for sample A

most of the precipitated Si is in crystalline form, while for samples with larger precipitates, a significant volume fraction of the precipitated Si is in amorphous form. A similar conclusion was drawn by Iacona *et al.*, after a comparison of dark field TEM and EFTEM analyses of similar layers.[18] This different structure can explain the variation observed in Fig. 4 and show that the refractive index of Si-nc in those composites depends more strongly on the crystalline or amorphous nature/content of the precipitates rather than on the size of the nanostructures, for the range of sizes used in this study.

IV. CONCLUSIONS

In conclusion, we have reported the experimental determination of the complex refractive index of Si-nc embedded in SiO_2 as a function of Si excess in the layer and Si-nc mean size, which is a fundamental requirement for waveguide design with these optically active composites. Assuming a Bruggeman modeling for the mixing of Si-nc and SiO_2 phases, we have obtained the refractive index of Si-nc, which is much lower than the one of amorphous and crystalline bulk Si. The absolute values of the refractive index depend strongly on the crystallized fraction of precipitated Si.

ACKNOWLEDGMENTS

This work was supported by the project SINERGIA (European Contract No. IST-2000-29650) and the Spanish National Project No. TIC2003-07464.

[1] G. Franzò *et al.*, Appl. Phys. A: Mater. Sci. Process. **74**, 1 (2002).
[2] L. Pavesi, L. Dal Negro, C. Mazzoleni, G. Franzò, and F. Priolo, Nature (London) **408**, 440 (2000).
[3] M. H. Nayfeh, S. Rao, and N. Barry, Appl. Phys. Lett. **80**, 121 (2002).
[4] F. Priolo, G. Franzò, F. Iacona, D. Pacifici, and V. Vinciguerra, Mater. Sci. Eng., B **81**, 9 (2001).
[5] H. S. Han, S. Y. Seo, and J. H. Shin, Appl. Phys. Lett. **79**, 4568 (2001).
[6] C. Q. Sun, X. W. Sun, B. K. Tay, H. T. Huang, and S. Li, J. Phys. D **34**, 3470 (2001).
[7] M. Lannoo, C. Delerue, and G. Allan, Phys. Rev. Lett. **74**, 3415, (1995).
[8] S. Charvet, R. Madelon, F. Gourbilleau, and R. Rizk, J. Appl. Phys. **85**, 4032 (1999).
[9] S. Charvet, R. Madelon, and R. Rizk, Solid-State Electron. **45**, 1505 (2001).
[10] D. Amans, S. Callard, A. Gagnaire, J. Joseph, G. Ledoux, and F. Huisken, J. Appl. Phys. **93**, 4173 (2003).
[11] B. Garrido, M. López, O. González, A. Pérez-Rodríguez, J. R. Morante, and C. Bonafos, Appl. Phys. Lett. **77**, 20 (2000).
[12] B. Garrido, M. López, C. García, A. Pérez-Rodríguez, J. R. Morante, C. Bonafos, M. Carrada, and A Claverie, J. Appl. Phys. **91**, 2 (2002).
[13] P. Pellegrino *et al.*, J. Appl. Phys. **97**, 74312 (2005).
[14] D. A. G. Bruggeman, Ann. Phys. **24**, 636 (1935).
[15] B. Abeles and J. I. Gittleman, Appl. Opt. **15**, 10 (1976).
[16] P. Y. Yu and M. Cardona, *Fundamentals of Semiconductors, Physics and Materials Properties* (Springer, Berlin, 1996).
[17] G. Dalba *et al.*, Appl. Phys. Lett. **82**, 889 (2003).
[18] F. Iacona, C. Bongiorno, C. Spinella, S. Boninelli, and F. Priolo, J. Appl. Phys. **95**, 3723 (2004).